A switch in kappa opioid receptor signaling from inhibitory to excitatory induced by stress in a subset of cortically-projecting dopamine neurons

Elyssa B. Margolis[1*]

[1]UCSF Weill Institute for Neurosciences, Neuroscience Graduate Program, Department of Neurology, University of California, San Francisco, CA, United States

*Corresponding Author

Email: Elyssa.Margolis@ucsf.edu

Abstract

The kappa opioid receptor (KOR) has shown potential as a therapeutic target for several neuropsychiatric disorders including major depressive disorder, pain, and substance use disorder. *In vivo* signaling of G protein coupled receptors like the KOR is generally thought to change in magnitude but not sign in such behavior states. Here we investigated KOR modulation of ventral tegmental area (VTA) neurons following an acute, behaviorally aversive manipulation. We found this switches KOR signaling from inhibitory to excitatory in a subset of VTA dopamine neurons. Brief corticotrophin releasing factor (CRF) exposure *ex vivo* rapidly induces a similar switch in KOR signaling, specifically in dorsal medial prefrontal cortex (dmPFC) projecting neurons, but not nucleus accumbens or basolateral amygdala projecting neurons. These KOR mediated excitations depend on G protein activation, but where somatodendritic VTA KORs activate a K^+ conductance to hyperpolarize dopamine neurons in control conditions, depolarizations require HCN channel function. One behavioral impact of this change is a loss of the aversiveness of intra-VTA KOR activation, providing direct evidence that rapid changes in GPCR signaling pathways can be triggered by activity at other GPCRs and significantly alter behavioral responses driven by neuromodulators.

Introduction

Activation of the KOR system mediates immediate processing of and long-lasting behavioral changes in response to aversive stimuli. Pharmacological blockade or genetic inactivation of KORs can decrease the acute aversiveness of stressors, including pain, and promote resilience to the development of depressive-like behaviors including decreased food reward seeking, decreased social interactions, and increased immobility in forced swim and social defeat paradigms[1–4]. Therefore, KOR antagonism has been proposed as a therapeutic approach to neuropsychiatric disorders with symptom profiles that include aversive emotional and anhedonic states, such as anxiety and depression, and to mitigate stress induced relapse to drug use[5].

The opioid receptor family of GPCRs commonly signals via inhibitory $G\alpha_{i/o}$ activation[6]. Agonists at somatodendritic KORs hyperpolarize neurons in a variety of brain regions including the dorsal raphe, nucleus raphe magnus, and ventral pallidum[7–9]. In the VTA, KOR activation inhibits a subset of dopamine neurons through G protein-gated inwardly rectifying K^+ channel (GIRK) activation while non-dopamine neurons show no response[10]. Behaviorally, KOR activation in the VTA is aversive[11], and intra-VTA blockade of KORs prevents the aversiveness of systemic KOR agonist administration[12]. Intra-VTA KOR blockade also prevents stress induced reinstatement of cocaine seeking[13]. Paradoxically, aversive stress blunts some physiological KOR responses, such as the KOR coupled GIRK conductance in serotonergic dorsal raphe neurons[8]. Understanding KOR function in relevant behavior states will improve our ability to treat the target neuropsychiatric disorders.

Here we investigated postsynaptic KOR agonist responses in VTA neurons after an acute aversive stressor in order to improve our understanding of what functionality KOR antagonism might have in a therapeutically relevant state. Rather than a change in response magnitude, acute aversive stress caused a change in the sign of the physiological response to KOR activation in a subset of VTA neurons. Importantly, this change was specific to VTA dopamine neurons projecting to the dmPFC, a site where dopamine function contributes to executive function and reward processing[14–17].

Results

45 We performed *ex vivo* whole cell recordings in rat VTA neurons after a single session of
46 aversive foot shock stress, making slices 30-60 min after the stressor. All statistics are
47 described in Table 1. In addition to VTA neurons that responded to the KOR selective agonist
48 U69,593 (1 μM) with a hyperpolarization or no change in membrane potential, similar to prior
49 observations in untreated animals[10,18,19], we unexpectedly observed depolarizations in a distinct
50 subset of neurons from both male and female rats (Fig. 1a-d). This includes neurons confirmed
51 as dopaminergic with immunocytochemistry (Fig. 1b, Supplementary Fig. 1a; recording
52 locations in Supplementary Fig. 1b). Depolarizations were still observed 3 (4/18 neurons), but
53 not 5 (0/7 neurons), days after the foot shock stress session (Fig 1d). Action potential (AP)
54 threshold was more depolarized in neurons from foot shock stressed rats compared to shams,
55 but did not alter other basal properties of VTA neurons including baseline input resistance (Ri),
56 AP duration, AP peak, h current magnitude, or spontaneous firing rate (Supplementary Fig. 2).
57 In the recordings from stressed animals, initial Ri was greater in neurons that subsequently
58 showed a depolarization in response to U69,593 compared to neurons that subsequently
59 showed a hyperpolarization (Supplementary Fig. 3). No other differences were detected in
60 baseline physiological properties across VTA neurons grouped by their U69,593 responses
61 (Supplementary Fig. 3). One possibility is that the aversive stressor decreases GIRK function in
62 a subset of neurons, unmasking the observed depolarizing effect of U69,593. However, when
63 we blocked GIRKs in slices from control, untreated animals with $BaCl_2$ (100 μM), the distribution
64 of responses to U69,593 was clearly different from those from stressed animals with no
65 depolarization > 0.8 mV (Fig. 1d,e). Dopamine D2 receptor activation hyperpolarizes a subset of
66 VTA neurons through GIRK channel activation[20]. If acute, aversive stress decreases GIRK
67 function in VTA neurons rather than change KOR signaling, we would expect to observe a shift
68 in responses to the D2R agonist quinpirole (1 μM) as well. The means and distributions of
69 quinpirole responses were not different between VTA neurons from sham and foot shocked rats
70 (Fig. 1f).

71 The corticotrophin releasing factor (CRF) system is upstream of the KOR system in encoding
72 the aversiveness of stressful experiences[21], and blocking the KORs can prevent CRF-induced
73 anxiety-like behaviors[22,23]. As foot shock stress drives CRF release in the VTA[24], we tested the
74 hypothesis that incubating VTA slices from control animals with no behavioral manipulations in
75 CRF would produce similar changes in KOR signaling to the *in vivo* aversive stressor exposure.
76 In fact, in VTA slices incubated in 200 nM CRF for 5 min, a subset of neurons responded to
77 subsequent U69,593 application with a depolarization (Fig. 2a). Next we tested whether
78 neurons excited by KOR activation after CRF were the same neurons inhibited by KOR
79 activation under control conditions or a previously KOR-insensitive population. All neurons that
80 showed a depolarization in response to KOR activation after CRF showed a hyperpolarization to
81 KOR activation before CRF (Fig. 2b,c). In fact, for neurons that showed a depolarization after
82 CRF, there was a clear inverse correlation (n = 5 neurons; coeff. = -0.9) between the
83 magnitudes of KOR responses before and after CRF application (Fig. 2c).

84 We previously reported that VTA dopamine neurons that project to the mPFC and basolateral
85 amygdala (BLA), but not the nucleus accumbens (NAc), are inhibited by somatodendritic KOR
86 activation in rat[18,19]. To test whether the signaling switch happens in a projection selective
87 manner, we recorded from retrogradely labeled VTA neurons that project to dmPFC (including
88 prelimbic and anterior cingulate cortices), ventral mPFC (infralimbic cortex), medial NAc, and
89 BLA blind to injection site. Most distinctly, dmPFC-projecting VTA neurons showed the strongest
90 depolarizations after CRF exposure while none of the vmPFC-projecting neurons depolarized
91 (Fig. 3). NAc- and BLA-projecting showed no and minimal depolarizations, respectively (Fig. 3).
92 Thus, the switch in KOR signaling from inhibitory to excitatory in a specific subpopulation of
93 dmPFC-projecting VTA neurons.

Next we probed the signaling mechanism underlying the KOR mediated excitations triggered by CRF exposure. To test whether the KOR excitations are due to indirect effects involving local connectivity in the slice we measured KOR agonist responses while blocking AMPARs (DNQX, 10 μM), $GABA_A$Rs (gabazine 20 μM), and action potential activity (500 nM TTX). This did not prevent U69,593 induced depolarizations (Fig. 4a). To block G protein signaling in the recorded neuron we included GDP-β-s in the intracellular solution (500 μM), and broke in to whole cell configuration only after CRF application was completed. This G protein block eliminated both depolarizations and hyperpolarizations induced by U69,593 (Fig. 4a). Together these data show that the KOR induced depolarizations are not circuit dependent, and because the G protein blockade was limited to the recorded neuron the KORs in question appear to be expressed in the recorded neuron. GPCR activation could cause depolarization by closing GIRKs[25], however blocking GIRKs with $BaCl_2$ (100 μM) did not prevent U69,593 induced depolarizations (Fig. 4a). We previously reported that mu and delta opioid receptors (MORs and DORs) on VTA neurons can drive depolarizations that require Ca^{2+} channel conductances[26,27], however in the present study, blocking Ca^{2+} channels with bath application of $CdCl_2$ (100 μM) did not prevent U69,593 induced depolarizations (Fig. 4a). A Na^+ leak current contributes to the maintenance of a depolarized potential and spontaneous AP firing in VTA neurons[28,29] that can be inhibited by $G\alpha_{i/o}$ protein coupled receptors[30]. Blocking this conductance did not prevent U69,593 induced depolarizations (Fig. 4a).

I_h is a hyperpolarization activated, non-selective cation conductance that we found is prominent in mPFC-projecting VTA neurons[19]. In nodose ganglion neurons MOR activation inhibits I_h[31], and in the nucleus raphe magnus (NRM) KOR activation augments I_h[32]. The I_h blocker ZD7288 prevented U69,593 induced depolarizations (Fig. 4a). Given that the reversal potential for I_h is depolarized compared to typical membrane potentials, the simplest possibility is that KOR activation augments I_h conductance. Consistent with this, we found that U69,593 increased I_h amplitude in a subset of neurons recorded in slices pretreated with CRF, and this response that was not observed in control slices (Fig. 4b). CRF pretreatment did not impact other I_h properties measured during U69,593 application (Supplementary Fig. 4).

Bruchas et al. reported that P38 MAPK contributes to some KOR mediated behavioral changes following aversive stressors *in vivo*[33]. Here we tested for a contribution of p38 to this KOR switch or KOR signaling. Incubating slices from control rats with the p38 blocker SB203580 prior to CRF application prevented subsequent U69,593 induced depolarizations (Fig. 4c). However, when slices were exposed to CRF prior to incubation in SB203580, U69,593 induced depolarizations persisted (Fig. 4a). We conclude that CRF receptor activation alters the signaling of a subset of KORs in the VTA through a p38 dependent signaling pathway, but KORs are not signaling through p38 directly to depolarize neurons.

Finally, we tested for a behavioral consequence of this change in KOR signaling. Decreases in dopamine neuron activity canonically encode punishment and aversion, and therefore intra-VTA KOR agonist induced aversion is widely thought to be due to inhibition of dopamine neurons. In the context of this model, a switch in KOR signaling in dopamine neurons from inhibitory to excitatory would be predicted to diminish conditioned place aversion (CPA) to intra-VTA KOR agonist microinjection. Since we found the switch in signaling sign to last between 3 and 5 days, we designed a paradigm where the animals received foot shock on days 1 and 6 in order to maintain stress-induced changes to KOR signaling. Pairings of either intra-VTA U69,593 (0.2 mM, 0.5 mL/side) or vehicle once per day were performed on non-stress days, for a total of four pairings per side (Fig. 5a), in order to minimize the formation of a direct association between the foot shock stress and the place preference manipulation. Indeed, foot shock stress pretreatment

eliminated the development of CPA to intra-VTA U69,593 (Fig. 5b, placements in Supplementary Fig. 5).

Discussion

Together, these data show that a single stressful event can dramatically change the signaling sign of a modulatory GPCR system. The change occurs in a specific neural circuit and can persist for days. This stress induced switch at KORs can also be induced by the stress-associated CRF neuropeptide-GPCR system in the same brain region, and while the signaling is still G protein mediated, It appears that the key conductance involved is I_h, a switch from GIRK coupling.

The contributions of VTA dopamine neurons to the processing of aversive experiences encompass motivational and learning components and are circuit-specific[34]. *In vivo* electrophysiology studies show that while many midbrain putative and opto-tagged dopamine neurons decrease their firing when a predicted reward is omitted (i.e., an aversive outcome)[34,35], some putative and directly identified dopamine neurons increase their firing in response to an aversive sensory stimulus[36,37]. We previously demonstrated that in control rats, KOR activation inhibits VTA dopamine neurons that project to the mPFC and BLA, but not the NAc[18,19]. With microdialysis, we confirmed that *in vivo* VTA KOR activation decreases dopamine release in mPFC but not in the NAc[19]. Here we show a switch from inhibitory to excitatory signaling in a subpopulation of dmPFC-projecting VTA neurons after CRF exposure. This excitatory KOR effect may contribute to the reported stress induced activation of dmPFC-projecting VTA dopamine neurons[35,36]. The loss of intra-VTA KOR agonist induced CPA after the stress induced switch in KOR signaling also implicates the dopaminergic projection to dmPFC in value signaling. Consistent with this, MOR activation in the VTA causes an increase in dopamine in the anterior cingulate cortex (ACC, included in the dmPFC in this study), and lesioning dopamine terminals there decreases the magnitude of intra-VTA MOR agonist induced conditioned place preference[15]. Also, genetic deletion of KOR from TH neurons prevents stress induced augmentation of cocaine CPP[37]. The transfer function of dopamine activity in the mPFC has been extensively studied, but a synthesized understanding of its contributions to mPFC processing remains somewhat elusive[38–40].

There are at least a dozen possible sources of CRF input to the VTA including the bed nucleus of the stria terminalis, dorsal raphe, parabrachial nucleus, lateral dorsal tegmentum, and local VTA neurons[41,42] that might be activated by aversive stressors. A subset of VTA neurons express CRF receptor 1 (CRF-R1) and the CRF binding protein, but not CRF receptor 2[43,44]. Blocking CRF-R1 in the VTA decreases foot shock stress induced reinstatement of cocaine seeking[35]. Further, intra-VTA KOR blockade[13] and intra-dmPFC dopamine antagonists also mitigate stress induced reinstatement of cocaine seeking[35,45], a provocative parallel to the neuromodulatory circuit identified here.

We found that blocking I_h prevented KOR agonist induced depolarizations. Even though I_h is generated by hyperpolarization activated, cyclic nucleotide-gated (HCN) channels[46,47] and thus opioid receptors might interact with them though cAMP modulation, in the NRM KOR activation in tissue from control rats augments I_h through a cAMP-independent signaling pathway that involves intracellular release of Ca^{2+} [32]. In these neurons, cAMP activation causes a positive shift in the voltage dependence of I_h, but does not change the maximum I_h amplitude. In the VTA, the adenylyl cyclase activator forskolin causes a depolarizing shift in the I_h $V_{1/2}$[48]. The isoform HCN3, which is expressed in the vast majority of VTA dopamine neurons and in many more VTA neurons than isoforms 1, 2 or 4[48], is relatively insensitive to cAMP[46,49]. Here, KOR activation after CRF did not alter I_h $V_{1/2}$, consistent with a cAMP-independent effect.

Consistent with our observations here, an increase in HCN channel function in the VTA has been implicated in behavioral changes induced by aversive stressors. For instance, after social defeat stress in mice, I_h magnitude is larger in VTA neurons of susceptible mice compared to those in control mice[50]. Blocking I_h in the VTA[50,51] and systemically[52] reverse the social avoidance induced by social defeat. Our data suggest that *in vivo* activity at KOR in the VTA after stress increases I_h function in dmPFC-projecting dopamine neurons. Thus decreasing I_h function in the VTA may be one common therapeutic target, be it through direct HCN blockade or by KOR antagonism.

What are the *in vivo* consequences of this switch in KOR signaling? At the circuit level, this change in KOR signaling means that the change in VTA dmPFC-projecting dopamine neuron firing will have an opposite sign when an endogenous KOR ligand is released into the VTA. That is, the peptidergic inputs to the VTA may have the same behaviorally related firing patterns as before an aversive stressor, but the impact on dmPFC dopamine release will be the inverse. In addition to contributing to value encoding, dopamine function in the dmPFC also contributes to executive function in several ways[16,17]. For instance, dopamine lesions in in the ACC impairs attentional set shifting[41] and dopamine receptor antagonists delivered to the prelimbic cortex degrade decision making[42]. These and other studies therefore suggest that ongoing or increases in dopamine release in the dmPFC contribute to saliency processing, and support working memory[43], which are particularly advantageous following an aversive stressor. Activating mPFC-projecting VTA dopamine neurons reverses chronic stress induced immobility and loss of sucrose preference[44], and an increase in dopamine signaling in dmPFC also relieves ongoing pain[45]. Provocatively, stress induced analgesia is also blocked by systemic administration of the KOR selective antagonist norBNI[46], which in the context of our results would prevent an increase in dopamine release in the dmPFC, although it is not yet known if dmPFC-projecting VTA dopamine neurons contribute to this phenomenon. Together, these studies raise the possibility that this switch in VTA KOR function is adaptive. An optimal concentration of dopamine in the mPFC facilitates learning, and learning about acutely aversive experiences, and how to avoid them, is critical to survival. Here we discovered a convergence of two neuropeptide systems, one changing the sign of the physiological response of the other in a specific neural circuit.

Methods

Animals.

All experiments were performed in accordance with the guidelines of the National Institutes of Health Guide for the Care and Use of Laboratory Animals and the Institutional Animal Care and Use Committees (IACUC) at the University of California San Francisco. Male and female Sprague Dawley rats were obtained from Inotiv or Charles River Laboratories. Rats were allowed access to food and water ad libitum and maintained on a reverse 12 h:12 h light/dark cycle. Rats were group housed except those with cannula implants.

Foot shock stress.

Operant chambers equipped with a foot shock grid were used for administering aversive stressors (physical boxes manufactured by Med. Associates with custom updated electronics controlled by microcontroller (Arduino)). Foot shock or sham sessions were 10 min, delivering 10, 0.8 mA intensity, 0.5 s duration shocks. Intervals between shocks were randomized (10 – 110 sec) in order to avoid predictability. Foot shock stress moderately elevated blood CORT, samples taken directly after foot shock session (Supplementary Fig. 6).

Electrophysiology.

236 Rats were deeply anesthetized with isoflurane, decapitated, and brains were quickly removed
237 and cooled with ice-cold artificial cerebrospinal fluid (aCSF) consisting of (in mM): 119 NaCl, 2.5
238 KCl, 1.0 NaH_2PO_4, 26.2 $NaHCO_3$, 11 glucose, 1.3 $MgSO_4$, 2.5 $CaCl_2$, saturated with 95% O_2-5%
239 CO_2, with a measured osmolarity 310–320 mOsm/L. Horizontal sections (150 µm) containing
240 the VTA were cut with a Leica VT 1000 S or a Campden 7000smz-2 vibratome. Tissue
241 containing the DiI injection sites was drop fixed in 4% formaldehyde to confirm targeting, with
242 recordings in DiI labeled neurons made blind to injection target. Slices were incubated in
243 oxygenated aCSF at 33 °C and allowed to recover for at least one hour. A single slice was
244 placed in the recording chamber and continuously superfused with oxygenated aCSF (2
245 mL/min). Neurons were visualized with an upright microscope (Zeiss AxioExaminer.D1)
246 equipped with infrared-differential interference contrast, Dodt optics, and fluorescent
247 illumination. Whole-cell recordings were made at 34 °C using borosilicate
248 glass microelectrodes (3–5 MΩ) filled with K-gluconate internal solution containing (in mM): 123
249 K-gluconate, 10 HEPES, 8 NaCl, 0.2 EGTA, 2 MgATP, 0.3 Na_3GTP, and 0.1% biocytin (pH 7.2
250 adjusted with KOH; 275 mOsm/L). Liquid junction potentials were not corrected. Input
251 resistance was monitored throughout voltage clamp experiments with a −4 mV step
252 every 30 s.
253 Signals were recorded using an Axopatch 1D (Molecular Devices, San Jose, CA) or IPA (Sutter
254 Instruments, Novato, CA). Signals were filtered at 5 kHz and collected at 20 kHz using IGOR
255 Pro (Wavemetrics) and custom data acquisition routines or collected at 10 kHz using
256 SutterPatch software (Sutter Instruments).
257 Baseline hyperpolarization-activated cation currents (I_h) were recorded in each neuron by
258 voltage clamping cells at -60 and stepping to -40, -50, -70, -80, -90, -100, -110, and -120 mV.
259 Recordings were then made in current clamp mode (I = 0 pA). Changes in I_h properties were
260 measured in voltage clamp, alternating between two step series (Supplementary Fig. 4) with
261 one series commencing each 2.17 min.
262 After recordings, slices were drop fixed in 4% PFA for at least 2 h at 4 °C and processed
263 for tyrosine hydroxylase (TH) immunocytochemistry and biocytin labeling. Recording were made
264 from throughout the VTA.
265
266 **Immunocytochemistry.**
267 Slices were preblocked for 2 h at room temperature in PBS with 0.3% Tween20 and 5% normal
268 goat serum, then incubated at 4°C with a rabbit anti-TH polyclonal antibody (1:400; EMD
269 Millipore, RRID: AB_390204). Slices were then washed thoroughly in PBS with 0.3% Tween20
270 before being agitated overnight at 4°C with Cy5 anti-rabbit secondary antibody (1:1000; Jackson
271 ImmunoResearch, RRID: AB_2534032) and FITC streptavidin (1:200; Jackson
272 ImmunoResearch, AB_2337236). Tween20 was excluded in slices with DiI. Sections were
273 rinsed and mounted on slides using VECTASHIELD® Antifade Mounting Media (Vector
274 Laboratories) and visualized with an Axioskop FS2 Plus (Zeiss) with an Axiocam MRm (Zeiss)
275 running Neurolucida (MBF Biosciences).
276
277 **CORT ELISA.**
278 Trunk blood was collected at time of slice preparation for electrophysiology animals. Samples
279 were centrifuged, then serum was frozen and stored at -80°C. ELISA kits were used as directed
280 (DetectX Corticosterone Enzyme Immunoassay Kit (product # K014-H1); Arbor Assays).
281
282 **Stereotaxic surgeries.**
283 *Tracer injections.* Rats weighing 275–300 g were anesthetized with 3–5% isoflurane (Henry
284 Schein) via inhalation and secured in a stereotaxic frame. Bilateral craniotomies were created
285 with a dental drill above the injection site.
286

Tracer injections. Bilateral injections of DiI (7% in ethanol; Biotium, Hayward, CA) were made in the dmPFC (2.0 mm AP, ± 0.6 mm ML, -2.8 mm V), vmPFC (2.0 mm AP, ± 0.6 mm ML, -4.8 mm V), NAc (1.2 mm AP, ± 0.8 mm ML, -7.4 mm V), or amygdala (-3.3 mm AP, ± 5.0 mm ML, -8.4 mm V) using a Nanoject II (Drummond Scientific, Broomall, PA). 50 – 300 nL was injected in each hemisphere over ~5 min. The injector tip was left in place for at least 2 minutes after injection to decrease backflow and spread to tissue dorsal to the injection site. Recordings were made 7-8 days later.

Cannulation. For microinjections into the VTA, bilateral guide cannulae were implanted 1 mm above the VTA (−5.8 mm AP, ±0.5 mm ML,−7.2 mm DV). A dummy stylet was inserted to maintain patency of the cannulae. Cannulae were anchored with flat point screws and dental cement.

Analgesia and recovery. Rats were treated with subcutaneous Carprofen (5 mg/kg, Zoetis) and topical 2% lidocaine (Phoenix Pharmaceutical, Inc.) during the surgery for pain control. After surgery, animals had access to liquid Tylenol (~1:40) in their drinking water for 3–5 days or were administered Meloxicam (s.c. 2 mg/kg, Pivetal) once per day for two days. All DiI and cannulae placements were histologically verified postmortem.

Conditioned place preference.

Rats were allowed to recover for 1–2 weeks prior to behavioral testing. First, all rats were tested for bias in the conditioning boxes. The conditioning boxes (physical boxes purchased from Med. Associates, Georgia, VT, USA with custom updated electronics (Arduino; IR beam breaks (Adafruit)) and software have three divisions: two conditioning chambers (25 cm × 21 cm × 21 cm) with distinct visual (horizontal vs. vertical stripes) and textural (thick vs. thin mesh flooring) cues, separated by a smaller gray neutral chamber (12 cm × 21 cm × 21 cm). Animals were allowed up to three opportunities to show neutrality across the chambers during 20-min baseline sessions. Rats that displayed a consistent baseline preference (>65% of time spent in one chamber) were excluded from the study. Rats were pseudorandomly assigned to receive U69,593 in one of the conditioning chambers, and assignments were counter-balanced for each cohort.

The paradigm commenced with a foot shock or sham treatment as described above, completed in a different room from the conditioning chambers. Starting the next day, conditioning pairings (20 min) occurred once daily for 4 consecutive days alternating U69,593 (0.2 mM) and vehicle (0.5 mL/side). This 5 day series (including foot shock/sham) was repeated a second time for a total of 4 pairings for U69,593 and vehicle, each. Finally, on test day, rats were drug free and had access to all three chambers for 20 min. Difference score was defined as (Time spent in U69,593 paired chamber)−(Time spent in vehicle paired chamber).

Microinjections. Rats were lightly restrained in a cloth wrap for intracranial microinjections. A bilateral 33 G microinjector (PlasticsOne) that extended 1 mm ventrally beyond the guide cannula was inserted to deliver drug. Hamilton syringes were driven by a dual syringe pump to deliver the injection volume over 2 min. Injectors were left in place for 1 min after injection.

Brain removal and histochemistry. To check cannulae placements, rats were deeply anesthetized with an intraperitoneal injection of Euthasol (0.1 mg/kg, Virbac Animal Health) after 0.3 µL of Chicago Sky Blue (in 2% PBS) was injected through the cannulae to mark injection locations. After becoming unresponsive to noxious stimuli, the rats were transcardially perfused with 400 mL of saline, followed by 400 mL of 4% paraformaldehyde (PFA) in 0.1 M phosphate buffer. The brains were extracted and immersion-fixed in PFA for 2 h at room temperature (RT), washed two times with PBS to remove excess PFA, and stored in 1X PBS at 4°C.

Perfused brains and drop fixed DiI containing tissue were sectioned (50 µm) using a vibratome (Leica VT 1000S). Alternating slices were Nissl stained. Sections were mounted on slides using VECTASHIELD® mounting medium (Vector Laboratories). Microinjection locations for rats included in the behavior study are summarized in Supplementary Fig. 5.

Data analysis.

The magnitude of U69,593 induced changes in V_m were quantified by comparing the mean values over the last 4 min of U69,593 application to the 4 minutes of baseline just prior to starting the drug application. Responses were tested for significance by statistically comparing 30 sec bins during these two time periods (unpaired Student's t-test). I_h magnitude was measured as the difference between the initial capacitive response to a voltage step from −60 to −120 mV and the final current during the same step. Reported baseline Ri and firing rate are the average measurements over the first 2 min of I_{clamp} recording. For AP duration measurements, at least 8 waveforms were averaged together and duration was calculated from threshold on the ascending phase to recrossing threshold on the falling phase. Threshold was identified as the first datapoint where the derivative of the waveform exceeds 10 V/s. For evaluation of KOR agonist induced changes in I_h properties, see measurements described in Supplementary Fig. 4.

Population statistics were performed in R. Where datasets failed tests of normality or homogeneity of variance, non-parametric permutation analyses (https://github.com/eb-margolis-neuroscience-lab/R-general-Margolislab/tree/main) were used to test for statistical significance. For behavior data, mixed measures two way ANOVA was used with Bonferroni correction for multiple comparisons.

Acknowledgements

I thank Joseph R. Driscoll, Thomas J. Cirino, Peter Fong, Aashka Popat, Ben J. Ngu, Benjamin Snyder, Kasra Mansorian, and Madelyn Moulton for technical assistance. This work was supported by National Institutes of Health grants R01DA030529, R01DA042025 and R01DA008863, and funds from the State of California for medical research on alcohol and substance use.

Figure Captions

Figure 1. Following a single foot shock session, a subset of VTA neurons depolarize in response to KOR activation. (a) Rats experienced a single intermittent foot shock session (10 min) prior to *ex vivo* whole cell recordings. (b) Example recording from a VTA neuron (biocytin fill: red) that was confirmed as dopaminergic with TH immunocytochemistry (green), scale bar 10 μm. In whole cell current clamp configuration (I = 0 pA) bath application of the KOR agonist U69,592 (1 μM) caused a depolarization. Inset: I_h measured in voltage clamp, scale bars 200 pA and 200 ms. (c) Mean time course of responses in neurons that were significantly depolarized by U69,593. (d) Summarized data, each circle is a neuron, from same day sham shock, same day shock, 3 days after shock and 5 days after shock treated rats. Circles and triangles indicate VTA neurons from male and female rats, respectively. Permutation analysis comparing means of U69,593 responses in sham vs shock, p = 0.02 (Table 1) Shading indicates within cell statistics (inset) (e) Summarized U69,593 responses in VTA neurons from naïve rats, and from naïve rats where U69,593 responses were measured in $BaCl_2$ (100 μM). Statistical comparison performed was permutation analysis comparing variances (SDs; $ indicates p<0.05), p = 0.04. (f) Summarized responses to the dopamine D2 receptor agonist quinpirole (1 μM) in VTA neurons from naïve, sham, and foot shocked rats. One way ANOVA sham vs shock, p = 0.9.

Figure 2. *ex vivo* exposure to CRF can switch KOR signaling from inhibitory to excitatory. (a) Summarized data, each circle is a neuron. Slices were incubated for 5 min with CRF (200 nM), CRF was washed out for at least 5 min, then U69,593 (1 μM) was bath applied for 5 min. Statistical comparison to U69,593 responses in VTA neurons from naïve rats (Fig. 1e left), Permutation analysis of means, p = 0.00004. Shading indicates within cell statistics. (b) Left, U69,593 (1 μM) was applied once, washed out, then reapplied (paired t-test p = 1.0). Right, U69,593 (1 μM) was applied once, washed out, CRF was washed on (5 min, 200 nM), washed out, then U69,593 was reapplied (paired t-test p = 0.08). (c) Data from (b) graphed as magnitude of response to first U69,593 application to second application.

Figure 3. CRF switches KOR signaling in a subpopulation of dmPFC-projecting VTA neurons. U69,593 responses were recorded in retrogradely labeled neurons after slices were incubated in CRF (5 min, 200 nM). Kruskal-Wallis rank sum test p = 0.006, pairwise comparisons listed in Table 1. Shading indicates within cell statistics.

Figure 4. KOR mediated depolarizations require I_h. (a) Signaling mechanism(s) that contribute to U69,593 (1 μM) induced depolarizations were investigated after exposing slices *ex vivo* to CRF (5 min, 200 nM). TTX (500 nM), DNQX (10 μM), and gabazine (20 μM) blocked synaptic transmission; intracellular GDP-β-s (500 μM) blocked intracellular G protein signaling; $BaCl_2$ (100 μM) blocked K^+ channels; $CdCl_2$ (100 μM) blocked Ca^{2+} channels; replacement of Na^+ with NMDG (151 mM, replacing NaCl) in aCSF blocked Na^+ leak current; ZD7288 (10 μM) blocked HCN channels (I_h); SB203580 (10 μM) blocked p38/MAPK signaling. (b) I_h magnitude was measured during U69,593 (1 μM) application in voltage clamp, stepping from -60 mV to -120 mV, in control slices or slices pretreated with CRF (5 min, 200 nM). (c) p38/MAPK was blocked with SB203580 application during both CRF and U69,593 application. Shading indicates within cell statistics.

Figure 5. Foot shock stress eliminates intra-VTA KOR mediated aversion. (a) Experiment timeline where rats were trained in a conditioned place preference paradigm, to intra-VTA U69,593 (0.2 mM, 0.5 mL/side) or vehicle. Rats were pretreated with sham handling or foot shock stress on non-pairing days. (b) Baseline vs post test for place conditioning. Two way mixed measures ANOVA) Pairwise comparisons: Sham, baseline vs post test: 0.0004 Shock, baseline vs post test: 0.6 (Bonferroni corrected).

Supplementary Figure 1. (a) Summary of responses to U69,593 in neurons identified at TH(+) with immunocytochemistry. These are a subset of the data in Fig. 1d. (b) Locations of VTA neurons recorded from same day foot shock stress rats. Color indicates change in Vm in response to U69,593.

Supplementary Figure 2. Physiological properties recorded in VTA neurons from foot shock (same day) or sham rats. Quantifications of data collected during the first 150 s immediately after whole cell access is achieved. (a) Ri, (b) AP duration, (c) AP threshold, (d) AP peak, (e) I_h magnitude (f) spontaneous firing rate. $^{**}p < 0.01$

Supplementary Figure 3. Foot shock rat data from Supplementary Figure 2, sorted by the type of response to U69,593. (a) Ri, (b) AP duration, (c) AP threshold, (d) AP peak, (e) I_h magnitude $^{*}p < 0.05$

Supplementary Figure 4. I_h measurements. (a) top, schematic of V step commands from V=-40 mV to quantify $V_{1/2}$ and activation τ. Bottom, example response. (b) top, schematic of V step commands from V = -40 mV to quantify reversal V. Bottom, example response from the same

434 neuron as in (a). (c) Example single exponential fit to data in (a). (d) Schematic of experiment
435 design. Step series shown in (a) and (b) were applied to each neuron for a "baseline"
436 measurement and again during U69,593 application. (e) Difference between $V_{1/2}$ measured at
437 baseline and in U69,593. Grey is no pretreatment, Orange is CRF pretreatment. (f) Difference
438 between $V_{reverse}$ measured at baseline and in U69,593. Grey is no pretreatment, Orange is CRF
439 pretreatment. (g) I_h activation τ at baseline vs in U69,593. Grey is no pretreatment, Orange is
440 CRF pretreatment.

441 **Supplementary Figure 5.** Microinjection sites for intra-VTA place conditioning experiments in
442 Figure 5.

443 **Supplementary Figure 6.** CORT measured (ELISA) from trunk blood samples collected from
444 same day foot shock and sham animals during brain slice preparation. * p = 0.05

445 **References**

446 1. Varlinskaya, E. I., Spear, L. P. & Diaz, M. R. Stress alters social behavior and sensitivity to
447 pharmacological activation of kappa opioid receptors in an age-specific manner in
448 Sprague Dawley rats. *Neurobiol. Stress* **9**, 124–132 (2018).

449 2. McLaughlin, J. P., Li, S., Valdez, J., Chavkin, T. A. & Chavkin, C. Social defeat stress-
450 induced behavioral responses are mediated by the endogenous kappa opioid system.
451 *Neuropsychopharmacology* **31**, 1241–8 (2006).

452 3. Massaly, N. *et al.* Pain-Induced Negative Affect Is Mediated via Recruitment of The
453 Nucleus Accumbens Kappa Opioid System. *Neuron* (2019)
454 doi:10.1016/j.neuron.2019.02.029.

455 4. Groblewski, P. A., Zietz, C., Willuhn, I., Phillips, P. E. M. & Chavkin, C. Repeated stress
456 exposure causes strain-dependent shifts in the behavioral economics of cocaine in rats.
457 *Addict. Biol.* **20**, 297–301 (2015).

458 5. Carlezon Jr., W. A. & Krystal, A. D. Kappa-Opioid Antagonists for Psychiatric Disorders:
459 From Bench to Clinical Trials. *Depress. Anxiety* **33**, 895–906 (2016).

460 6. Reeves, K. C., Shah, N., Muñoz, B. & Atwood, B. K. Opioid Receptor-Mediated Regulation
461 of Neurotransmission in the Brain. *Front. Mol. Neurosci.* **15**, 919773 (2022).

462 7. Ji, M. *et al.* Dynorphin promotes stress-induced depressive behaviors by inhibiting
463 ventral pallidal neurons in rats. *Acta Physiol.* **236**, (2022).
464 8. Lemos, J. C. *et al.* Repeated stress dysregulates κ-opioid receptor signaling in the dorsal
465 raphe through a p38α MAPK-dependent mechanism. *J. Neurosci. Off. J. Soc. Neurosci.* **32**,
466 12325–12336 (2012).
467 9. Pan, Z. Z., Tershner, S. A. & Fields, H. L. Cellular mechanism for anti-analgesic action of
468 agonists of the kappa-opioid receptor. *Nature* **389**, 382–385 (1997).
469 10. Margolis, E. B., Hjelmstad, G. O., Bonci, A. & Fields, H. L. Kappa-opioid agonists directly
470 inhibit midbrain dopaminergic neurons. *J Neurosci* **23**, 9981–6 (2003).
471 11. Bals-Kubik, R., Ableitner, A., Herz, A. & Shippenberg, T. S. Neuroanatomical sites
472 mediating the motivational effects of opioids as mapped by the conditioned place
473 preference paradigm in rats. *J Pharmacol Exp Ther* **264**, 489–95 (1993).
474 12. Ehrich, J. M. *et al.* Kappa Opioid Receptor-Induced Aversion Requires p38 MAPK
475 Activation in VTA Dopamine Neurons. *J Neurosci* **35**, 12917–31 (2015).
476 13. Graziane, N. M., Polter, A. M., Briand, L. A., Pierce, R. C. & Kauer, J. A. Kappa opioid
477 receptors regulate stress-induced cocaine seeking and synaptic plasticity. *Neuron* **77**,
478 942–954 (2013).
479 14. Vijayraghavan, S., Major, A. J. & Everling, S. Neuromodulation of Prefrontal Cortex in
480 Non-Human Primates by Dopaminergic Receptors during Rule-Guided Flexible
481 Behavior and Cognitive Control. *Front. Neural Circuits* **11**, 91 (2017).
482 15. Narita, M. *et al.* Implication of dopaminergic projection from the ventral tegmental area
483 to the anterior cingulate cortex in μ-opioid-induced place preference. *Addict. Biol.* **15**,
484 434–447 (2010).

485 16. Tichelaar, J. G., Sayalı, C., Helmich, R. C. & Cools, R. Impulse control disorder in
486 Parkinson's disease is associated with abnormal frontal value signalling. *Brain J. Neurol.*
487 **146**, 3676–3689 (2023).
488 17. Cools, R., Froböse, M., Aarts, E. & Hofmans, L. Dopamine and the motivation of cognitive
489 control. *Handb. Clin. Neurol.* **163**, 123–143 (2019).
490 18. Margolis, E. B., Mitchell, J. M., Ishikawa, J., Hjelmstad, G. O. & Fields, H. L. Midbrain
491 dopamine neurons: projection target determines action potential duration and
492 dopamine D(2) receptor inhibition. *J Neurosci* **28**, 8908–13 (2008).
493 19. Margolis, E. B. *et al.* Kappa opioids selectively control dopaminergic neurons projecting
494 to the prefrontal cortex. *Proc Natl Acad Sci U A* **103**, 2938–42 (2006).
495 20. Seutin, V., Johnson, S. W. & North, R. A. Effect of dopamine and baclofen on N-methyl-D-
496 aspartate-induced burst firing in rat ventral tegmental neurons. *Neuroscience* **58**, 201–
497 206 (1994).
498 21. Land, B. B. *et al.* The dysphoric component of stress is encoded by activation of the
499 dynorphin kappa-opioid system. *J Neurosci* **28**, 407–14 (2008).
500 22. Bruchas, M. R., Land, B. B., Lemos, J. C. & Chavkin, C. CRF1-R activation of the
501 dynorphin/kappa opioid system in the mouse basolateral amygdala mediates anxiety-
502 like behavior. *PloS One* **4**, e8528 (2009).
503 23. Van't Veer, A., Yano, J. M., Carroll, F. I., Cohen, B. M. & Carlezon, W. A. Corticotropin-
504 releasing factor (CRF)-induced disruption of attention in rats is blocked by the κ-opioid
505 receptor antagonist JDTic. *Neuropsychopharmacol. Off. Publ. Am. Coll.*
506 *Neuropsychopharmacol.* **37**, 2809–2816 (2012).

507 24. Wang, B. *et al.* Cocaine experience establishes control of midbrain glutamate and
508 dopamine by corticotropin-releasing factor: a role in stress-induced relapse to drug
509 seeking. *J Neurosci* **25**, 5389–96 (2005).
510 25. Xia, Y.-F., Margolis, E. B. & Hjelmstad, G. O. Substance P inhibits GABAB receptor
511 signalling in the ventral tegmental area. *J. Physiol.* **588**, 1541–1549 (2010).
512 26. Margolis, E. B., Hjelmstad, G. O., Fujita, W. & Fields, H. L. Direct bidirectional μ-opioid
513 control of midbrain dopamine neurons. *J Neurosci* **34**, 14707–16 (2014).
514 27. Margolis, E. B., Fujita, W., Devi, L. A. & Fields, H. L. Two delta opioid receptor subtypes
515 are functional in single ventral tegmental area neurons, and can interact with the mu
516 opioid receptor. *Neuropharmacology* **123**, 420–432 (2017).
517 28. Cobb-Lewis, D. E., Sansalone, L. & Khaliq, Z. M. Contributions of the Sodium Leak
518 Channel NALCN to Pacemaking of Medial Ventral Tegmental Area and Substantia Nigra
519 Dopaminergic Neurons. *J. Neurosci. Off. J. Soc. Neurosci.* **43**, 6841–6853 (2023).
520 29. Khaliq, Z. M. & Bean, B. P. Pacemaking in dopaminergic ventral tegmental area neurons:
521 depolarizing drive from background and voltage-dependent sodium conductances. *J.*
522 *Neurosci. Off. J. Soc. Neurosci.* **30**, 7401–7413 (2010).
523 30. Philippart, F. & Khaliq, Z. M. Gi/o protein-coupled receptors in dopamine neurons
524 inhibit the sodium leak channel NALCN. *eLife* **7**, e40984 (2018).
525 31. Ingram, S. L. & Williams, J. T. Opioid inhibition of Ih via adenylyl cyclase. *Neuron* **13**,
526 179–186 (1994).
527 32. Pan, Z. Z. κ-Opioid receptor-mediated enhancement of the hyperpolarization-activated
528 current (Ih) through mobilization of intracellular calcium in rat nucleus raphe magnus.
529 *J. Physiol.* **548**, 765–775 (2003).

530 33. Bruchas, M. R. *et al.* Stress-induced p38 mitogen-activated protein kinase activation
531 mediates kappa-opioid-dependent dysphoria. *J Neurosci* **27**, 11614–23 (2007).
532 34. Morales, M. & Margolis, E. B. Ventral tegmental area: cellular heterogeneity,
533 connectivity and behaviour. *Nat Rev Neurosci* (2017) doi:10.1038/nrn.2016.165.
534 35. Vranjkovic, O. *et al.* Enhanced CRFR1-Dependent Regulation of a Ventral Tegmental
535 Area to Prelimbic Cortex Projection Establishes Susceptibility to Stress-Induced
536 Cocaine Seeking. *J. Neurosci. Off. J. Soc. Neurosci.* **38**, 10657–10671 (2018).
537 36. Deutch, A. Y. *et al.* Stress selectively increases fos protein in dopamine neurons
538 innervating the prefrontal cortex. *Cereb. Cortex N. Y. N 1991* **1**, 273–292 (1991).
539 37. Abraham, A. D., Casello, S. M., Land, B. B. & Chavkin, C. Optogenetic stimulation of
540 dynorphinergic neurons within the dorsal raphe activate kappa opioid receptors in the
541 ventral tegmental area and ablation of dorsal raphe prodynorphin or kappa receptors
542 in dopamine neurons blocks stress potentiation of cocaine reward. *Addict. Neurosci.* **1**,
543 100005 (2022).
544 38. Sheynikhovich, D., Otani, S., Bai, J. & Arleo, A. Long-term memory, synaptic plasticity and
545 dopamine in rodent medial prefrontal cortex: Role in executive functions. *Front. Behav.*
546 *Neurosci.* **16**, 1068271 (2023).
547 39. Durstewitz, D. & Seamans, J. K. The dual-state theory of prefrontal cortex dopamine
548 function with relevance to catechol-o-methyltransferase genotypes and schizophrenia.
549 *Biol. Psychiatry* **64**, 739–749 (2008).
550 40. Robinson, S. E. & Sohal, V. S. Dopamine D2 Receptors Modulate Pyramidal Neurons in
551 Mouse Medial Prefrontal Cortex through a Stimulatory G-Protein Pathway. *J. Neurosci.*
552 *Off. J. Soc. Neurosci.* **37**, 10063–10073 (2017).

553 41. Soden, M. E. *et al.* Distinct Encoding of Reward and Aversion by Peptidergic BNST
554 Inputs to the VTA. *Front. Neural Circuits* **16**, 918839 (2022).
555 42. Grieder, T. E. *et al.* VTA CRF neurons mediate the aversive effects of nicotine
556 withdrawal and promote intake escalation. *Nat. Neurosci.* **17**, 1751–1758 (2014).
557 43. Van Pett, K. *et al.* Distribution of mRNAs encoding CRF receptors in brain and pituitary
558 of rat and mouse. *J. Comp. Neurol.* **428**, 191–212 (2000).
559 44. Wang, H.-L. & Morales, M. Corticotropin-releasing factor binding protein within the
560 ventral tegmental area is expressed in a subset of dopaminergic neurons. *J. Comp.*
561 *Neurol.* **509**, 302–318 (2008).
562 45. McFarland, K. & Kalivas, P. W. The circuitry mediating cocaine-induced reinstatement of
563 drug-seeking behavior. *J. Neurosci. Off. J. Soc. Neurosci.* **21**, 8655–8663 (2001).
564 46. Combe, C. L. & Gasparini, S. Ih from synapses to networks: HCN channel functions and
565 modulation in neurons. *Prog. Biophys. Mol. Biol.* **166**, 119–132 (2021).
566 47. Monteggia, L. M., Eisch, A. J., Tang, M. D., Kaczmarek, L. K. & Nestler, E. J. Cloning and
567 localization of the hyperpolarization-activated cyclic nucleotide-gated channel family in
568 rat brain. *Mol. Brain Res.* **81**, 129–139 (2000).
569 48. Mu, L. *et al.* cAMP-mediated upregulation of HCN channels in VTA dopamine neurons
570 promotes cocaine reinforcement. *Mol. Psychiatry* **28**, 3930–3942 (2023).
571 49. Mistrík, P. *et al.* The Murine HCN3 Gene Encodes a Hyperpolarization-activated Cation
572 Channel with Slow Kinetics and Unique Response to Cyclic Nucleotides. *J. Biol. Chem.*
573 **280**, 27056–27061 (2005).

50. Cao, J.-L. *et al.* Mesolimbic dopamine neurons in the brain reward circuit mediate susceptibility to social defeat and antidepressant action. *J. Neurosci. Off. J. Soc. Neurosci.* **30**, 16453–16458 (2010).

51. Cai, M. *et al.* HCN channel inhibitor induces ketamine-like rapid and sustained antidepressant effects in chronic social defeat stress model. *Neurobiol. Stress* **26**, 100565 (2023).

52. Teichman, E. M. *et al.* Design and validation of novel brain-penetrant HCN channel inhibitors to ameliorate social stress-induced susceptible phenotype. *Mol. Psychiatry* (2025) doi:10.1038/s41380-025-02972-8.

Table 1 – Assumption testing and statistical comparisons for summary data						
Experiment	**Figure**	**# Neurons; # Outliers; # Extreme outliers**	**Shapiro-Wilk test of Normality Statistic; p val**	**Test for Homogeneity of Variances Statistic; p val (Test used)**	**Parametric test Statistic; p val (Test used)**	**Non-parametric test Statistic and/or p val (Test used)**
U69,593 response (mV), acute stress vs sham	1d	67; 3; 0	0.9; 0.00008	7.5; 0.008 (Levene's)	n/a	0.02 (Permutation, mean)
U69,593 response in $BaCl_2$ vs acute stress	1d,e	49; 4; 0	0.9; 0.0007	3.0; 0.09 (Levene's)	n/a	0.04 (Permutation, SD)
Quinpirole response (mV), acute stress vs sham	1f	27; 2; 1	1.0; 0.6	1.4; 0.2 (Levene's)	0.02; 0.9 (one way ANOVA)	n/a
U69.593 response naïve vs after CRF	1e, 2a	78; 2; 0	1.0; 0.02	0.9; 0.4 (Levene's)	n/a	0.00004
U69,593, first application vs second application	2b, left	6; 0; 0	0.9; 0.6	0.02; 0.9	0.0003; 1.0 (paired t-test)	
U69,593 responses pre- vs post- CRF	2b, right	10; 0; 0	1.0; 0.7	2.0; 0.2	-2.0; 0.08 (paired t-test)	
U69,593, first application vs second application	2c	6; 0; 0			5.1; 0.007 (Pearson's product moment correlation, coeff = 0.9)	
U69,593 responses pre- vs post- CRF, in neurons with a post-CRF U69,593 induced depolarization	Subset in 2c	5			-3.7; 0.03 (Pearson's product moment correlation, coeff = -0.9)	
U69,593 responses differ by projection target	3	48; 6; 3	0.8; 0.0000001	1.4; 0.3	n/a	12.4; 0.006 (Kruskal-Wallis rank sum test) Pairwise comparisons (p adjustment method BH): dmPFC-BLA: 0.05 dmPFC-NAc: 0.05 dmPFC-vmPFC: 0.03 BLA-NAc: 0.4 BLA-vmPFC: 0.4 NAc-vmPFC: 0.2
U69,593 after CRF vs after CRF with GDP-β-s	4a	34; 1; 0	0.9; 0.007	4.4; 0.05	n/a	0.01 (Permutation, SD)
U69,593 after CRF vs after CRF with ZD7288	4a	39; 2; 1	0.9; 0.06	2.5; 0.1	0.7; 0.4 (one way ANOVA)	
U69,593 after CRF vs after CRF with TTX, DNQX, gabazine	4a	47; 4; 0	0.9; 0.005	1.2; 0.3	n/a	0.3 (Permutation, mean)
U69,593 after CRF vs after CRF with $BaCl_2$	4a	38; 1; 0	0.9; 0.01	2.5; 0.1	n/a	0.5 (Permutation, mean)
U69,593 after CRF vs after CRF with $CdCl_2$	4a	33; 1; 0	0.9; 0.007	0.01; 0.9	n/a	0.6 (Permutation, mean)
U69,593 after CRF vs after CRF with NMDG	4a	31; 1; 0	0.9; 0.01	1.1; 0.3	n/a	0.2 (Permutation, mean)
U69,593 after CRF vs after CRF with SB203580 (only during U69,593)	4a	36; 1; 0	0.9; 0.00008	7.5; 0.008	n/a	0.4 (Permutation, mean)
I_h magnitude after U69,593, with vs without CRF pretreatment	4b	18; 2; 0	0.9; 0.02	1.7; 0.2	n/a	0.3 (Permutation, mean)
U69,593 after CRF vs after CRF with SB203580 (applied	4a,c	34; 2; 0	1.0; 0.2	0.0007; 1.0	3.8; 0.06	

during CRF and U69,593)						
Intra-VTA U69,593 place conditioning, sham- vs shock-treated rats	5b	20 rats; 0; 0	Base-sham: 1.0; 0.8 Base-shock: 0.9; 0.6 Sham-test: 0.9; 0.5 Shock-test: 0.9; 0.4	Sham: 0.9; 0.4 Shock: 3.5; 0.08	Pretreatment-U69,593 interaction: 9.0; 0.008 (Two way mixed measures ANOVA) Pairwise comparisons: Sham, Base vs test: 0.0004 Shock, Base vs test: 0.6 (Bonferroni corrected)	
Baseline Ri in neurons from stress vs sham animals	Supp 2	139; 0; 0	1.0; 0.01	0.5; 0.5		0.2 (Permutation, mean)
Spontaneous AP duration in neurons from stress vs sham animals	Supp 2	81; 1; 0	0.9; 0.00002	0.9; 0.3		0.8 (Permutation, mean)
Spontaneous AP threshold in neurons from stress vs sham animals	Supp 2	81; 0; 0	1.0; 0.8	0.9; 0.3	9.5; 0.003 (one way ANOVA)	
Spontaneous AP peak in neurons from stress vs sham animals	Supp 2	81; 1; 0	1.0; 0.09	1.5; 0.2	0.2; 0.7 (one way ANOVA)	
I_h magnitude in neurons from stress vs sham animals	Supp 2	129; 17; 10	0.6; <0.000001	0.5; 0.5		0.4 (Permutation, mean)
Baseline spontaneous firing rate in neurons from stress vs sham animals	Supp 2	60; 5; 3	0.8; <0.000001	0.4; 0.5		0.3 (Permutation, mean)
Proportion of spontaneously active neurons from stress vs sham animals						0.9 (two tailed Fisher exact test)
Baseline Ri in neurons from stress animals grouped by U69,593 response type	Supp 3	46; 0; 0	1.0; 0.4	0.2; 0.8	3.2; 0.04 (one way ANOVA) Pairwise comparisons: Inhib-excit: 0.04 Inhib-no resp: 0.2 Excit-no resp: 0.9	
AP duration in neurons from stress animals grouped by U69,593 response type	Supp 3	27; 0; 0	0.9; 0.1	4.4; 0.02		3.1; 0.2 (Kruskal-Wallis rank sum test)
AP threshold in neurons from stress animals grouped by U69,593 response type	Supp 3	27; 0; 0	1.0; 0.4	1.5; 0.2	0.3; 0.7 (one way ANOVA)	
AP peak in neurons from stress animals grouped by U69,593 response type	Supp 3	27; 1; 0	0.9; 0.1	0.6; 0.5	0.8 (one way ANOVA)	

CORT from recording animals, foot shock vs sham	Supp 6	16 rats; 1; 0	0.9; 0.2	0.09; 0.8	0.05 (one way ANOVA)	

Figure 1

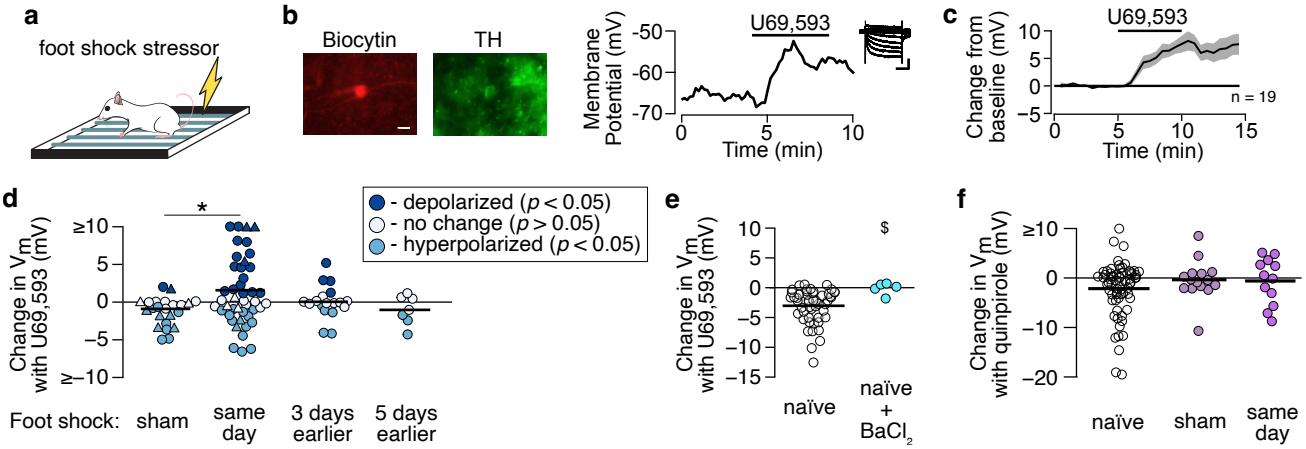

Figure 2

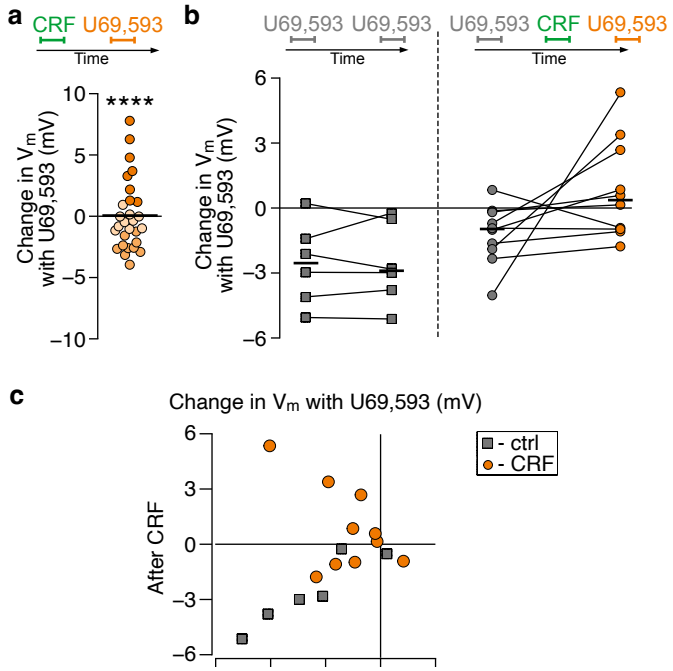

Figure 3

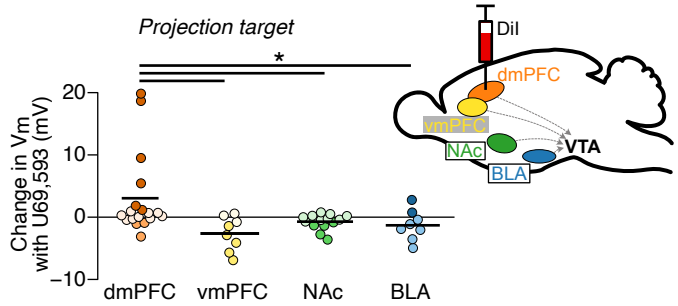

Figure 4

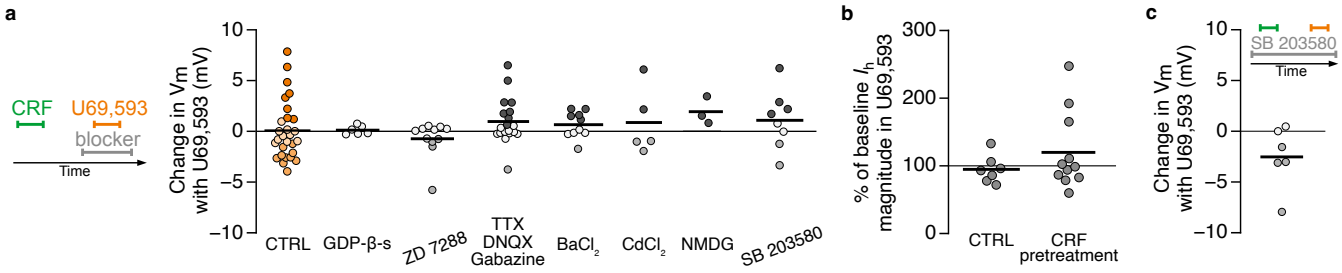
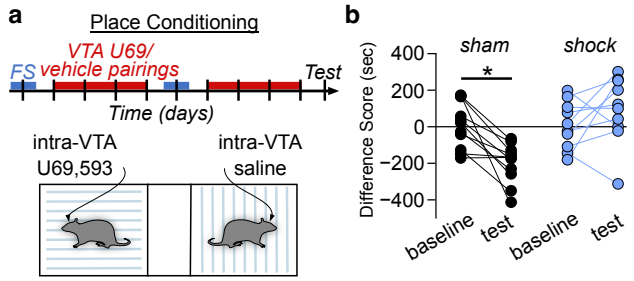
Figure 5